JACS
JOURNAL OF THE AMERICAN CHEMICAL SOCIETY

Communication

pubs.acs.org/JACS

End-On Orientation of Semiconducting Polymers in Thin Films Induced by Surface Segregation of Fluoroalkyl Chains

Jusha Ma,[†,‡] Kazuhito Hashimoto,[‡] Tomoyuki Koganezawa,[§] and Keisuke Tajima*[,∥,⊥]

[†]School of Material Science and Engineering, Beijing Institute of Technology, 5 South Zhongguancun Street, Haidian District, Beijing 100081, China

[‡]Department of Applied Chemistry, School of Engineering, The University of Tokyo, 7-3-1 Hongo, Bunkyo-ku, Tokyo 113-8656, Japan

[§]Japan Synchrotron Radiation Research Institute, 1-1-1 Kouto, Sayo-cho, Sayo-gun, Hyogo 679-5198, Japan

[∥]Precursory Research for Embryonic Science and Technology, Japan Science and Technology Agency, 4-1-8 Honcho, Kawaguchi, Saitama 332-0012, Japan

[⊥]RIKEN Center for Emergent Matter Science (CEMS), 2-1 Hirosawa, Wako, Saitama 351-0198, Japan

Supporting Information

ABSTRACT: Controlling the orientation of highly anisotropic structures of polymers is important because the majority of their mechanical, electronic, and optical properties depend on the orientation of the polymer backbone. In thin films, the polymer chains tend to adopt an orientation parallel to the substrate; therefore, forcing the chains to stand perpendicular to the substrate is challenging. We have developed a simple way to achieve this end-on orientation. We functionalized one end of a poly(3-butylthiophene) (P3BT) chain with a 1*H*,1*H*,2*H*,2*H*,3*H*,3*H*-perfluoroundecyl group, which caused spontaneous self-segregation of the polymer (P3BT-F_{17}) to the surface of the polymer film. In P3BT-F_{17}/polystyrene (PS) blend films, a highly ordered end-on orientation of the conjugated backbone was observed in the surface-segregated layer of the crystalline P3BT-F_{17}. Furthermore, when the film was spin-coated from a mixture of P3BT-F_{17} and P3BT, the chain orientation of P3BT-F_{17} at the surface forced the P3BT in the bulk of the film to adopt the end-on orientation because of the high crystallinity of P3BT. The electronic conductivity measured perpendicular to the film surface also reflected the end-on orientation in the bulk, resulting in a more than 30-fold enhancement of the hole mobility.

Regioregular poly(3-alkylthiophene) (P3AT) has attracted intense interest over the last two decades as a p-type semiconductor with high charge mobility due to its high crystallinity and large absorption coefficient in the visible region. For P3AT, it is known that an edge-on orientation (Figure 1b) is better suited to organic field-effect transistors (OFETs)[1,2] than the face-on orientation (Figure 1d), because the charge transport in OFETs is parallel to the surface and is better in the $\pi-\pi$ stacking direction (along the *b* axis) than in the alkyl-side-chain direction (along the *a* axis).[3] In contrast, the direction of the charge transport is perpendicular to the substrate in polymer solar cells (PSCs);[4−6] therefore, the face-on orientation is more suitable than the edge-on orientation. This is consistent with studies of various planar semiconducting polymers in PSCs.[7−9] Because the intramolecular electronic coupling is much larger than the intermolecular coupling in the crystal structure, the intramolecular charge transport along the polymer main chains (*c* axis) may be much faster than in the other two directions (*a* and *b* axes).[10] Therefore, achieving the end-on orientation of the polymer chains in the thin films (Figure 1c) would improve the charge transport perpendicular to the substrate. However, making the long polymer chains stand perpendicular to the substrate is quite a big challenge. Although there are a few examples of partial end-on orientations of semiconducting polymers, which have been achieved with polymer brushes grown from the substrate surface,[11] nanoimprinting,[12] nanopores,[13] etched nanostructures,[14] or solvent-vapor treatment,[15] the end-on orientation in entire thin films has never been achieved. If simple methods such as spin-coating can induce the chain orientation, it could be applicable to many electronic devices based on polymer thin films.

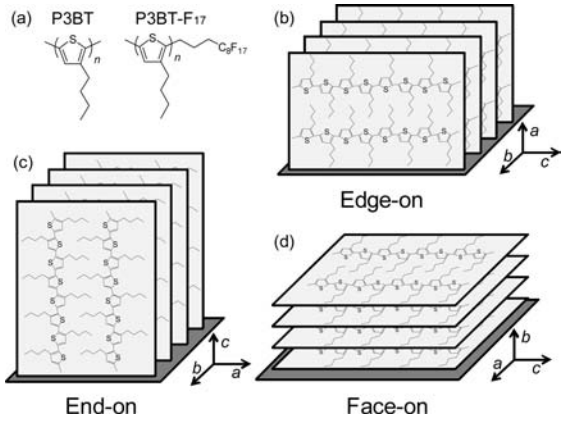

Figure 1. (a) Molecular structures of P3BT and P3BT-F_{17}. (b−d) Schematic representations of (b) edge-on, (c) end-on, and (d) face-on orientations in P3BT thin films.

Received: May 22, 2013
Published: June 19, 2013

dx.doi.org/10.1021/ja4051179 | *J. Am. Chem. Soc.* 2013, 135, 9644−9647

Fluoroalkyl groups have a low surface energy and tend to self-segregate to the air−liquid interface during film formation.[16] We recently showed that adding fluoroalkylated semiconducting materials to the coating solution could be a useful method for modifying the film surface of organic semiconducting materials. We called them surface-segregated monolayers (SSMs) and used the dipole moment of the fluoroalkyl chains to manipulate the electronic properties of organic semiconducting films and bilayer PSCs.[17] In this study, we formed an SSM using poly(3-butylthiophene) (P3BT) with one chain end functionalized with a 1*H*,1*H*,2*H*,2*H*,3*H*,3*H*-perfluoroundecyl group (Figure 1a). The fluoroalkyl group at the chain end of the resulting polymer (P3BT-F_{17}) self-segregated to the surface, which aligned the P3BT backbone perpendicular to the surface and produced the maximum surface coverage. In addition, because of the high crystallinity of P3BT, the surface orientation induced polymer chains in the bulk of the film to adopt the same orientation, as confirmed by X-ray photoelectron spectroscopy (XPS), XPS depth profiles, and grazing-incidence X-ray diffraction (GIXRD). The optical anisotropy of the films was examined by UV−vis absorption with linearly polarized light. The charge transport properties in the perpendicular direction were investigated by space-charge-limited current (SCLC) measurements.

The surface segregation behavior in films spin-coated from P3BT-F_{17}/P3BT or P3BT-F_{17}/polystyrene (PS) solutions was investigated by XPS. The highest coverage of the fluoroalkyl chain on the film surface was estimated to be >90% on the basis of the difference between the observed and calculated F/C ratios [see Figure S1 in the Supporting Information (SI) for details of the calculation].[18,19] XPS depth profile and angle-dependent XPS measurements indicated that during the spin-coating process, P3BT-F_{17} spontaneously self-segregated to the film surface as a monolayer, with P3BT or PS forming the bulk of the film underneath (Figures S2 and S3).

The crystalline structure and chain orientation of P3BT in the thin films were determined by out-of-plane and in-plane GIXRD measurements.[20−22] Depending on the chain orientation of P3BT (Figure 1), diffraction peaks from the lamellar structure repeating along the *a* axis and the $\pi-\pi$ stacking along the *b* axis should be visible in either the out-of-plane or in-plane measurements. The incident angle (ω) was fixed at 0.2°.[23,24] Figure 2a,b shows out-of-plane and in-plane GIXRD patterns, respectively, of P3BT films spin-coated onto a silicon substrate. The films were annealed after spin-coating to promote crystallization of the polymers. The diffraction patterns of the P3BT films can be attributed to the edge-on orientation (Figures 1b and 2c), which is usually observed for P3AT thin films because of the hydrophobic interactions between the alkyl chains and the substrate.[25,26] The lower surface energy of the alkyl side chains may also induce the edge-on orientation at the surface during spin-coating.[27,28]

The GIXRD patterns for the P3BT-F_{17}/PS films were significantly different than those of the P3BT films. Because PS is an amorphous polymer, the diffraction peaks from P3BT-F_{17}/PS should be from crystalline P3BT-F_{17}.[25] Peaks were observed only in the in-plane scan. The two peaks at 6.8° (13.0 Å) and 13.6° (6.5 Å) were assigned to the (100) and (200) diffractions from the lamellar structure, respectively. In the $\pi-\pi$ stacking region, there were two peaks at 23.4° (3.8 Å) and 24.3° (3.7 Å). These peaks were also observed in the same region in the powder XRD patterns of pristine P3BT-F_{17} and P3BT, which is consistent with previous studies.[29] This suggests that there are two possible $\pi-\pi$ stacking arrangements for P3BT with slightly

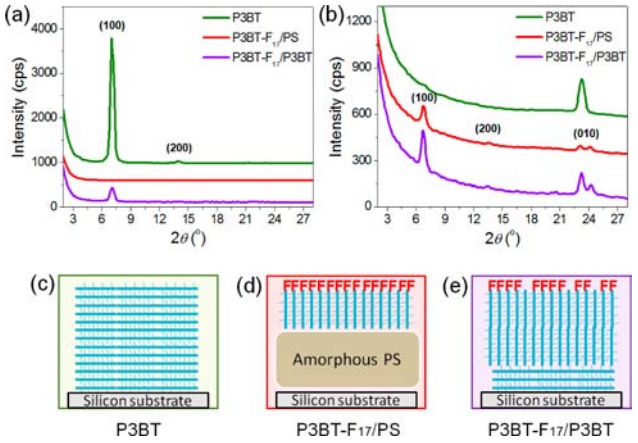

Figure 2. (a) Out-of-plane and (b) in-plane GIXRD scans of P3BT and P3BT-F_{17}/PS films. The patterns have been shifted in the *y* direction for ease of comparison. (c−e) Schematic representations of (c) P3BT, (d) P3BT-F_{17}/PS, and (e) P3BT-F_{17}/P3BT films. The blue rods represent P3BT, and the red "F"s represent the fluoroalkyl chains.

different distances. The reason for the difference between the powder and thin-film patterns of P3BT is still unclear, but it might be due to the effect of the substrate or differences in the crystallization conditions.[30] Nevertheless, the absence of peaks in the out-of-plane scan and the presence of all of the peaks in the in-plane scan indicate that both the *a* and *b* axes of P3BT-F_{17} were oriented parallel to the substrate in the P3BT-F_{17}/PS films. This orientation was also clearly observed in the two-dimensional (2D) GIXRD pattern obtained using synchrotron radiation (Figure S4). These results suggest a structure in which the P3BT-F_{17} layer was segregated from the PS to the film surface and adopted an end-on orientation with good crystallinity (Figure 2d). The degree of polymerization (*n*) in P3BT-F_{17} was 18 on average, as estimated by MALDI-TOF mass spectrometry. With this value of *n*, the length of the backbone with a completely extended conformation was calculated from the molecular model to be 8 nm.

Next, we focused on the P3BT-F_{17}/P3BT film. Both the top P3BT-F_{17} layer and the P3BT in the film bulk could produce crystalline peaks. X-ray reflectivity (XRR) measurements indicated that the film thickness was 20.7 nm, which was comparable to that of the P3BT film (19.9 nm). The GIXRD patterns of the films are compared in Figure 2a,b. In the out-of-plane scan, the P3BT-F_{17}/P3BT film showed a (100) peak, although the intensity was significantly lower than for the P3BT film. The in-plane scan contained (100) and (200) peaks and two peaks in the $\pi-\pi$ stacking region, similar to that for the P3BT-F_{17}/PS film. This indicates that the edge-on and end-on orientations coexisted in the P3BT-F_{17}/P3BT film. The intensities of the lamellar peaks in the out-of plane scan were much weaker than those of a P3BT film with a similar thickness, although the peak intensities in the $\pi-\pi$ stacking region were similar. This suggests that in addition to the P3BT-F_{17} layer on the top, some of the P3BT in the bulk of the film may also adopt the end-on orientation.

The GIXRD patterns of the P3BT-F_{17}/P3BT film before and after thermal annealing showed that annealing enhanced the lamellar peaks in the in-plane scan and weakened them in the out-of-plane scan (Figure S5). This implies that the P3BT chains rearranged themselves into the end-on orientation during the annealing process. This rearrangement may have been induced by the P3BT-F_{17} groups at the surface of the film. However, the

dx.doi.org/10.1021/ja4051179 | *J. Am. Chem. Soc.* 2013, 135, 9644−9647

P3BT close to the substrate probably adopted an edge-on orientation because of the interactions with the substrate (Figure 2e).

The hypothesis that the end-on orientation at the surface induces the orientation inside the film was tested further by preparing P3BT-F_{17}/poly(3-hexylthiophene) (P3HT) films spin-coated from the blended solution. The different lengths of the alkyl side chains altered the *d* spacings of the P3HT lamellar structure compared with that of P3BT. Because the depth of the X-ray penetration into the films depends on ω,[31] the depth distribution of the P3BT and P3HT crystalline structures in the film was observed by changing ω. The in-plane GIXRD pattern was measured by gradually varying ω from 0.12°, which is lower than the critical angle for P3BT ($\alpha_c = 0.157°$ for $\lambda = 1.54$ Å[24]), to 0.18°, which is higher than the critical angle for P3HT (α_c = 0.158°) and lower than that for the silicon substrate ($\alpha_c = 0.23°$). Figure 3 shows that for $\omega < 0.16°$, only the P3BT lamellar peak

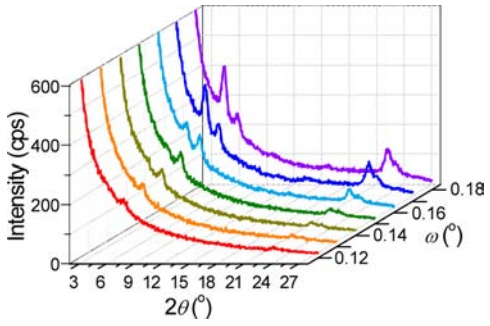

Figure 3. In-plane GIXRD patterns of the P3BT-F_{17}/P3HT film with incident angles (ω) from 0.12 to 0.18°.

was observed at 6.8° (13.0 Å). The P3HT lamellar peak at 5.3° (16.6 Å) began to appear as ω increased, indicating that P3HT was present inside the film. The peaks appeared in the in-plane scans, consistent with P3HT also adopting an end-on orientation in the film. These results imply that the end-on orientation formed in the top layer can induce the same orientation in the bulk of the film. In the out-of-plane scan of the P3BT-F_{17}/P3HT films (Figure S6), only the P3HT lamellar peak at 5.6° (15.8 Å) was observed, suggesting that P3HT also adopted the edge-on orientation at the interface with the substrate (Figure 2e).

We propose the following mechanism for the end-on orientation based on the XPS and GIXRD results. When the blended P3BT-F_{17}/P3BT solution is spin-coated onto the silicon substrate, the fluoroalkyl chains segregate to the surface of the liquid films. During the evaporation of the solvent, the P3BT group in P3BT-F_{17} begins to crystallize at the surface with an end-on orientation. Some of the P3BT also cocrystallizes with the same orientation, although the edge-on orientation is preferred at the interface with the substrate because of the hydrophobic interactions with the substrate. When the films are annealed, the disordered P3BT rearranges and adopts the end-on orientation induced by the P3BT-F_{17} at the film surface.

To elucidate the effect of the chain orientation on the optical anisotropy, UV–vis absorption spectra of the P3BT-F_{17}/PS and P3BT films were measured with linearly polarized light (Figure 4). Because PS is optically transparent, it was easier to observe the orientation anisotropic effects in P3BT-F_{17}/PS. At normal incidence (0°), the P3BT-F_{17}/PS film showed an absorption maximum at 480 nm, which was red-shifted compared with that of the $CHCl_3$ solution (445 nm). However, it was a much shorter

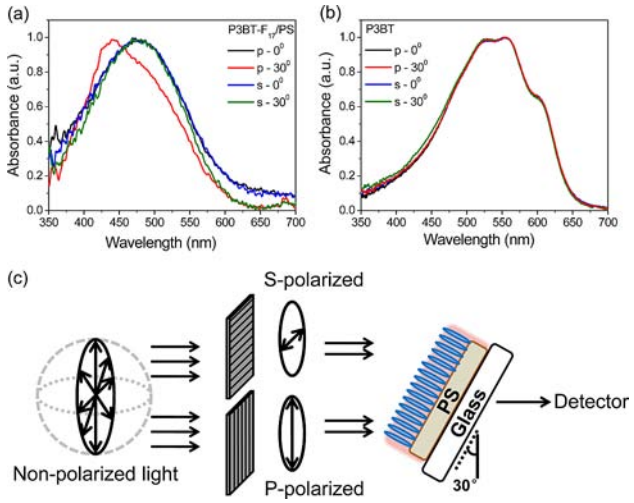

Figure 4. (a, b) Normalized UV–vis absorption spectra of (a) P3BT-F_{17}/PS and (b) P3BT films with s- and p-polarized light at different incident angles. (c) Setup for the polarized-light UV–vis measurements.

wavelength than that of the P3BT film, which had an absorption maximum at 525 nm with two shoulders at 555 and 605 nm. For both samples, identical spectra were produced using s- and p-polarized light, indicating a random 2D orientation in the plane. When the incident angle for the measurements was 30°, the absorption maximum of the p-polarized light was blue-shifted to 440 nm for the P3BT-F_{17}/PS film, whereas no change was observed with s-polarized light. This change indicates optical anisotropy perpendicular to the film surface. The P3BT film did not show any anisotropic effect (Figure 4b), as expected for the edge-on orientation. The blue shift for the P3BT-F_{17}/PS film was different from the red shift generally observed for crystalline P3AT films (Figure 4a). At first glance, one might think that this could be caused by the shorter effective conjugation length of the P3BT group, but this would not be consistent with the high crystallinity of P3BT-F_{17} observed by XRD. Our tentative explanation is the formation of H-aggregation in the P3BT layer,[32−34] because interchain interactions may occur in only the lateral direction. Further studies are necessary to elucidate the optical properties of the aggregation state in the films. In the previous reports, similar a blue shift was observed for a P3BT film and was attributed to the structural transition from form I to form II with a change in the π–π stacking distance from 3.8 to 4.4 Å.[35,36] In the current study, however, the stacking distance of 3.7–3.8 Å (form I) did not change with the orientation. Therefore, the blue shift in the P3BT-F_{17}/PS film does not originate from a change in the strength of the intermolecular interactions but probably results from a change in the manner of the intermolecular coupling as suggested above.

To elucidate the effect of the backbone orientation on the charge carrier mobility in the thin films, the hole mobilities in the P3BT and P3BT-F_{17}/P3BT films were measured by the SCLC method.[37] The hole mobility in P3BT-F_{17}/P3BT films was $(1.6 \pm 0.1) \times 10^{-3}$ cm^2 V^{-1} s^{-1}, which is more than 30-fold higher than the hole mobility in the pristine P3BT films $[(4.2 \pm 0.8) \times 10^{-5}$ cm^2 V^{-1} $s^{-1}]$ (Figure S8). These results suggest that the end-on orientation of the polymer chains enhanced the hole mobility perpendicular to the film surface. Because the X-ray analyses showed that the edge-on orientation was present at the interface with the substrate in the P3BT-F_{17}/P3BT films,

dx.doi.org/10.1021/ja4051179 | J. Am. Chem. Soc. 2013, 135, 9644–9647

achieving the end-on orientation in the whole film could enhance the mobility further.

In summary, we have shown that the surface segregation of fluoroalkyl groups attached to the chain end caused the P3BT-F_{17} polymer chain to adopt an end-on orientation and induced the chains inside the film to adopt the same orientation. This unique orientation showed characteristic optical properties and improved the hole mobility perpendicular to the film by more than 30-fold compared with the usual edge-on orientation. This strategy could be applied to other crystalline semiconducting polymers and has great promise for controlling the optical and electronic properties of polymer films.

Experimental details. P3BT-F_{17} and P3BT were synthesized as reported elsewhere.[38] The number-average molecular weights (M_n) of P3BT-F_{17}, P3BT, and P3HT were 3700, 4000 and 6000, respectively, as measured by gel-permeation chromatography on a Prominence system (Shimadzu) equipped with a UV detector. PS (M_n = 6000) was purchased from Tohso. The P3BT-F_{17}/P3BT films were prepared as follows. Clean silicon substrates were spin-coated with a mixture of P3BT-F_{17} (3.0 g/L) and P3BT (4.5 g/L) in $CHCl_3$ at a speed of 3000 rpm for 40 s. The films were thermally annealed at 70 °C for 8 h and subsequently at 165 °C for 2 h. X-ray photoelectron spectroscopy (XPS) was performed on an AXIS Ultra DLD spectrometer (Kratos Analytical Ltd.) with Al Kα radiation for all the measurements. XRD and XRR analyses were performed on a Smartlab X-ray diffractometer (Rigaku) using monochromatized Cu Kα radiation (λ = 0.154 nm) generated at 45 kV and 200 mA. UV−vis spectra were recorded on a Jasco V-670 UV−vis spectrometer with a polarizer. Current density−voltage (J−V) measurements were conducted on hole-only devices with a structure of ITO/PEDOT:PSS (30 nm)/polymer film/MoO_3 (5 nm)/Au (30 nm).

■ ASSOCIATED CONTENT

Supporting Information

Experimental details and additional data. This material is available free of charge via the Internet at http://pubs.acs.org.

■ AUTHOR INFORMATION

Corresponding Author

keisuke.tajima@riken.jp

Notes

The authors declare no competing financial interest.

■ ACKNOWLEDGMENTS

This research was supported by JST, PRESTO. J.S.M. thanks Prof. Wenhui Wu for his kind support and the Chinese Scholarship Council for financial support. The authors thank Prof. Hideaki Yokoyama at the University of Tokyo for helpful discussions and Dr. Itaru Osaka at RIKEN for help with GIXRD measurements. GIXRD experiments were performed at BL19B2 at SPring-8 with the approval of the Japan Synchrotron Radiation Research Institute (JASRI) (Proposal 2013A1634).

■ REFERENCES

(1) Ong, B. S.; Wu, Y.; Liu, P.; Gardner, S. *J. Am. Chem. Soc.* **2004**, *126*, 3378.

(2) Zaumseil, J.; Sirringhaus, H. *Chem. Rev.* **2007**, *107*, 1296.

(3) Sirringhaus, H.; Brown, P. J.; Friend, R. H.; Nielsen, M. M.; Bechgaard, K.; Langeveld-Voss, B. M. W.; Spiering, A. J. H.; Janssen, R. A. J.; Meijer, E. W.; Herwig, P.; de Leeuw, D. M. *Nature* **1999**, *401*, 685.

(4) Zhao, G.; He, Y.; Li, Y. *Adv. Mater.* **2010**, *22*, 4355.

(5) Thompson, B. C.; Fréchet, J. M. J. *Angew. Chem., Int. Ed.* **2008**, *47*, 58.

(6) Franz, P.; Roman, S. R.; Niyazi, S. S. *Adv. Funct. Mater.* **2003**, *13*, 85.

(7) Piliego, C.; Holcombe, T. W.; Douglas, J. D.; Woo, C. H.; Beaujuge, P. M.; Fréchet, J. M. J. *J. Am. Chem. Soc.* **2010**, *132*, 7595.

(8) Guo, J.; Liang, Y.; Szarko, J.; Lee, B.; Son, H. J.; Rolczynski, B. S.; Yu, L.; Chen, L. X. *J. Phys. Chem. B* **2010**, *114*, 742.

(9) Osaka, I.; Saito, M.; Mori, H.; Koganezawa, T.; Takimiya, K. *Adv. Mater.* **2012**, *24*, 425.

(10) Saeki, A.; Koizumi, Y.; Aida, T.; Seki, S. *Acc. Chem. Res.* **2012**, *45*, 1193.

(11) Senkovskyy, V.; Tkachov, R.; Beryozkina, T.; Komber, H.; Oertel, U.; Horecha, M.; Bocharova, V.; Stamm, M.; Gevorgyan, S. A.; Krebs, F. C.; Kiriy, A. *J. Am. Chem. Soc.* **2009**, *131*, 16445.

(12) Aryal, M.; Trivedi, K.; Hu, W. *ACS Nano* **2009**, *3*, 3085.

(13) Coakley, K. M.; Srinivasan, B. S.; Ziebarth, J. M.; Goh, C.; Liu, Y.; McGehee, M. D. *Adv. Funct. Mater.* **2005**, *15*, 1927.

(14) Zan, H. W.; Hsu, Y. H.; Meng, H. F.; Huang, C. H.; Tao, Y. T.; Tsai, W. W. *Appl. Phys. Lett.* **2012**, *101*, No. 093307.

(15) Lu, G.; Li, L.; Yang, X. *Adv. Mater.* **2007**, *19*, 3594.

(16) (a) Wang, J.; Mao, G.; Ober, C. K.; Kramer, E. J. *Macromolecules* **1997**, *30*, 1906. (b) Katano, Y.; Tomono, H.; Nakajima, T. *Macromolecules* **1994**, *27*, 2342. (c) El-Shehawy, A. A.; Yokoyama, H.; Sugiyama, K.; Hirao, A. *Macromolecules* **2005**, *38*, 8285. (d) Yokoyama, H.; Tanaka, K.; Takahara, A.; Kajiyama, T.; Sugiyama, K.; Hirao, A. *Macromolecules* **2004**, *37*, 939.

(17) (a) Tada, A.; Geng, Y. F.; Wei, Q.; Hashimoto, K.; Tajima, K. *Nat. Mater.* **2011**, *10*, 450. (b) Geng, Y. F.; Tajima, K.; Hashimoto, K. *Macromol. Rapid Commun.* **2011**, *32*, 1478. (c) Geng, Y. F.; Wei, Q. S.; Hashimoto, K.; Tajima, K. *Chem. Mater.* **2011**, *23*, 4257. (d) Wei, Q. S.; Nishizawa, T.; Tajima, K.; Hashimoto, K. *Adv. Mater.* **2008**, *20*, 2211.

(18) Ton-That, C.; Shard, A. G.; Bradley, R. H. *Langmuir* **2000**, *16*, 2281.

(19) Cumpson, P. J. *Surf. Interface Anal.* **2001**, *31*, 23.

(20) DeLongchamp, D. M.; Kline, R. J.; Fischer, D. A.; Richter, L. J.; Toney, M. F. *Adv. Mater.* **2011**, *23*, 319.

(21) Shin, M.; Kim, H.; Park, J.; Nam, S.; Heo, K.; Ree, M.; Ha, C.-S.; Kim, Y. *Adv. Funct. Mater.* **2010**, *20*, 748.

(22) Yang, H.; Shin, T. J.; Yang, L.; Cho, K.; Ryu, C. Y.; Bao, Z. *Adv. Funct. Mater.* **2005**, *15*, 671.

(23) Kim, J.; Ryba, E.; Bai, J. *Polymer* **2003**, *44*, 6663.

(24) Birkholz, M. *Thin Film Analysis by X-Ray Scattering*; Wiley-VCH: Weinheim, Germany, 2006; p 155.

(25) Joseph, R. K.; McGehee, M. D.; Toney, M. F. *Nat. Mater.* **2006**, *5*, 222.

(26) Veres, J.; Ogier, S.; Lloyd, G.; de Leeuw, D. *Chem. Mater.* **2004**, *16*, 4543.

(27) Hao, X. T.; Hosokai, T.; Mitsuo, N.; Kera, S.; Okudaira, K. K.; Mase, K.; Ueno, N. *J. Phys. Chem. B* **2007**, *111*, 10365.

(28) Wei, Q. S.; Miyanishi, S.; Tajima, K.; Hashimoto, K. *ACS Appl. Mater. Interfaces* **2009**, *1*, 2660.

(29) Qu, Y. P.; Li, L. G.; Lu, G. G.; Zhou, X.; Su, Q.; Xu, W. T.; Li, S. J.; Zhang, J. D.; Yang, X. N. *Polym. Chem.* **2013**, *3*, 3301.

(30) Buono, A.; Son, N. H.; Raos, G.; Gila, L.; Cominetti, A.; Catellani, M.; Meille, S. V. *Macromolecules* **2010**, *43*, 6772.

(31) Lim, G.; Parrish, W.; Ortiz, C.; Bellotto, M.; Hart, M. *J. Mater. Res.* **2011**, *2*, 471.

(32) Muntwiler, M.; Zhu, X. Y. *Phys. Rev. Lett.* **2007**, *98*, No. 246801.

(33) Spano, F. C. *Acc. Chem. Res.* **2010**, *43*, 429.

(34) Westenhoff, S.; Abrusci, A.; Feast, W. J.; Henze, O.; Kilbinger, A. F. M.; Schenning, A. P. H. J.; Silva, C. *Adv. Mater.* **2006**, *18*, 1281.

(35) Lu, G. H.; Li, L. G.; Yang, X. N. *Macromolecules* **2008**, *41*, 2062.

(36) Liu, J. G.; Sun, Y.; Gao, X.; Xing, R. B.; Zheng, L. D.; Wu, S. P.; Geng, Y. H.; Han, Y. C. *Langmuir* **2011**, *27*, 4212.

(37) Stallinga, P. *Electrical Characterization of Organic Electronic Materials and Devices*; Wiley: Cornwall, U.K., 2009; p 45.

(38) Ma, J. S.; Geng, Y. F.; Hashimoto, K.; Tajima, K. *Macromol. Chem. Phys.* **2013**, *214*, 1326.